

Asymmetric Anion- $\pi$  Catalysis on Perylenediimides

Chao Wang, François N. Mirois, Jiri Mareda, Naomi Sakai, and Stefan Matile\*

**Abstract:** Anion- $\pi$  catalysis, that is the stabilization of anionic transition states on  $\pi$ -acidic aromatic surfaces, has so far been developed with naphthalenediimides (NDIs). This report introduces perylenediimides (PDIs) to anion- $\pi$  catalysis. The quadrupole moment of PDIs (+23.2 B) is found to exceed that of NDIs and reach new records with acceptors in the core (+70.9 B), and their larger surface provides space to better accommodate chemical transformations. Unlike NDIs, the activity of PDI catalysts for enolate and enamine addition is determined by the twist of their  $\pi$  surface rather than their reducibility. These results, further strengthened by nitrate inhibition and circular dichroism spectroscopy, support an understanding of anion- $\pi$  interactions centered around quadrupole moments, i.e., electrostatic contributions, rather than redox potentials and charge transfer. The large PDI surfaces provide access to the highest enantioselectivities observed so far in anion- $\pi$  catalysis (96 % ee).

Anion- $\pi$  interactions occur on  $\pi$ -acidic aromatic surfaces with positive quadrupole moment  $Q_{zz}$ .<sup>[1]</sup> Complementary to the conventional cation- $\pi$  interactions,<sup>[2]</sup> they are much younger,<sup>[3]</sup> more challenging,<sup>[1]</sup> and much less used to create function.<sup>[4–6]</sup> As recent as 2013, anion- $\pi$  catalysis has been introduced explicitly, i.e., based on positive  $Q_{zz}$  and activity increasing with  $\pi$  acidity.<sup>[7]</sup> The general idea is to stabilize anionic transition states on  $\pi$ -acidic aromatic surfaces. By now, contributions from anion- $\pi$  interactions to enolate,<sup>[8]</sup> enamine,<sup>[9]</sup> and iminium<sup>[10]</sup> chemistry processes have been reported, anionic cascade processes generating cyclohexane rings with five chiral centers from achiral, acyclic starting materials have been realized on  $\pi$ -acidic surfaces,<sup>[10]</sup> and the first anion- $\pi$  enzymes have been made.<sup>[11]</sup> Apart from occasional, related observations in diverse functional systems,<sup>[12]</sup> explicit anion- $\pi$  catalysis has been realized on the  $\pi$ -acidic surface of naphthalenediimides (NDIs).<sup>[13]</sup> In this report, anion- $\pi$  catalysis is explored on perylenediimides (PDIs).<sup>[14]</sup> This is of interest because their  $\pi$  surface offers much needed space to accommodate organic transformations. Anion- $\pi$  interactions on PDIs are essentially unexplored. However, surprisingly fast reactions have been observed on PDIs early on,<sup>[15]</sup> initial Kemp eliminations have been tested on unsubstituted PDIs,<sup>[16]</sup> and anion- $\pi$  transport has been implied in electroneutral PDI photosystems.<sup>[17]</sup>

Quadrupole moments  $Q_{zz}$  of PDIs were calculated first following standard procedures (MP2/6-311G\*\*//M062X/6-311G\*\*).<sup>[18]</sup> We found a  $Q_{zz}$  = +23.2 B for PDIs with *N*-phenyl substituents for the imides and without core substituents. This finding was quite remarkable because already the  $Q_{zz}$  = +17.7 B of unsubstituted NDIs is twice the  $\pi$  acidity of the hexafluorobenzene standard.<sup>[4]</sup> The  $Q_{zz}$  of 1,6,7,12 or “*meta*” substituted PDIs could not be calculated easily because plane twisting breaks the symmetry. However, a spectacular  $Q_{zz}$  = +70.9 B was obtained for the planar, 2,5,8,11- or “*ortho*”-substituted tetracyano PDIs,<sup>[19]</sup> and contrary to the tetracyano NDIs ( $Q_{zz}$  = +55.0 B),<sup>[18]</sup> these “super- $\pi$ -acids” are synthetically accessible<sup>[20]</sup> (2,8-dicyano PDI:  $Q_{zz}$  = +46.5 B). Larger  $Q_{zz}$  for PDIs compared to NDIs were understandable considering that quadrupole moments increase with the number of valence electrons.<sup>[21]</sup> Together with the high polarizability of expanded  $\pi$  surfaces, these extraordinary  $Q_{zz}$  thus suggested that anion- $\pi$  interactions with PDIs could be very strong. Further modulation of their  $\pi$  acidity was envisioned with sulfide redox switches.<sup>[22]</sup> Upon oxidation from two “*meta*” sulfides to sulfoxides and sulfones in the PDI core, the energy of the LUMO level decreases from –4.00 eV to –4.32 eV and –4.40 eV, respectively (Table 1; 2,5,8,11-tetracyano PDI: –4.72 eV<sup>[20]</sup>).<sup>[22]</sup> This trend is similar to but not as pronounced as with NDIs.<sup>[22]</sup>

To explore anion- $\pi$  catalysis on PDI surfaces, we first focused on enamine addition (Figure 1). The addition of aldehyde **1** to nitroolefin **2** to yield product **3** with two stereogenic centers is of interest for anion- $\pi$  catalysis because it has been shown that the presence of a carboxylic acid near the proline is essential to shift the rate-limiting step from protonation of the nitronate intermediate to the C–C bond formation.<sup>[23]</sup> Stereoselective stabilization of this **TS1** on the compact, crowded  $\pi$ -acidic NDI surfaces by operational

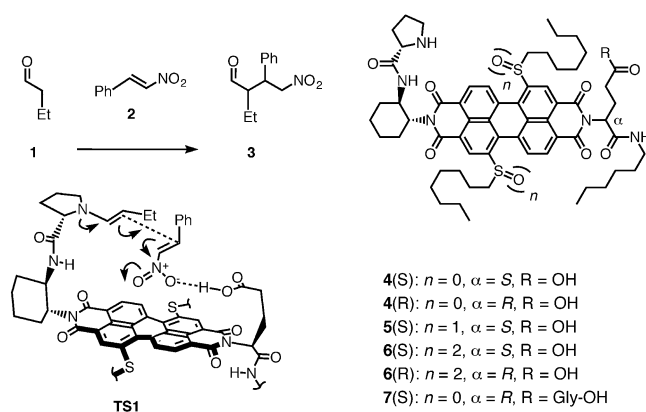


**Figure 1.** Anion- $\pi$  PDI catalysts **4–7** for the asymmetric addition to enamine acceptor **2**, and schematic representation of transition state **TS1**.

\* Dr. C. Wang, F. N. Mirois, Dr. J. Mareda, Dr. N. Sakai, Prof. S. Matile  
 Department of Organic Chemistry, University of Geneva  
 Geneva (Switzerland)  
 E-mail: stefan.matile@unige.ch  
 Homepage: <http://www.unige.ch/sciences/chior/matile/>

Supporting information and the ORCID identification number(s) for the author(s) of this article can be found under <http://dx.doi.org/10.1002/anie.201608842>.

**Table 1:** Key characteristics of PDI anion- $\pi$  catalysts.

Entry	Core <sup>[a]</sup>	$E_{\text{LUMO}}$ [eV] <sup>[b]</sup>	Cat. <sup>[d]</sup>	$\Delta\epsilon$ [M <sup>-1</sup> cm <sup>-1</sup> ] <sup>[e]</sup>	Enamine catalysis <sup>[c]</sup> $\Delta E_a$ [kJ mol <sup>-1</sup> ] <sup>[f]</sup>	<i>ee</i> [%] <sup>[g]</sup>	d.r. <sup>[h]</sup>	IC <sub>50</sub> [mM] <sup>[i]</sup>	Enolate catalysis <sup>[j]</sup> Cat. <sup>[k]</sup>	$\Delta E_a$ [kJ mol <sup>-1</sup> ] <sup>[l]</sup>	A/D <sup>[m]</sup>
1	SR	-4.00	4(S)	0 (0)	0 (0)	96 (69)	25:1 (16:1)	125	11	0	1.8
2			+ NO <sub>3</sub> <sup>-[n]</sup>		+ 3.13	31	10:1				
3			+ PF <sub>6</sub> <sup>-[o]</sup>		-0.18	92	14:1				
4			C <sub>6</sub> F <sub>6</sub> /C <sub>6</sub> D <sub>6</sub> <sup>[p]</sup>		-0.80	92	10:1				
5	SR		4(R)	0 (0)	+ 2.92 (+0.12)	73 (68)	22:1 (18:1)				
6	SR		7(R)		+ 1.66 (-1.40)	76 (68)	7:1 (10:1)				
7	SOR, <i>anti</i>	-4.32	5(S,F1)	+ 8 (-2)	+ 2.83 (+1.41)	87 (52)	19:1 (14:1)		12	+ 1.68	1.0
8	SOR, <i>anti</i>		5(S,F2)	+ 8 (+15)	+ 1.03 (+0.72)	89 (58)	15:1 (14:1)				
9	SOR, <i>syn</i>	-4.35	5(S,F3)	-22 (-50)	+ 1.55 (+1.41)	82 (50)	16:1 (12:1)				
10	SOR, <i>syn</i>		5(S,F4)	+ 38 (+40)	+ 0.61 (+1.23)	88 (60)	16:1 (15:1)				
11	SO <sub>2</sub> R	-4.40	6(S)	-25 (-8)	+ 0.48 (+0.56)	89 (59)	20:1 (18:1)	265	13	+ 2.22	0.6
12	SO <sub>2</sub> R		6(R)	-23 (-5)	+ 2.08 (+0.64)	82 (59)	18:1 (14:1)				

[a] Substituents in the PDI core (Figures 1 and 4). [b] Energy of the LUMO, determined by DPV in CH<sub>2</sub>Cl<sub>2</sub> against -5.10 eV for Fc/Fc<sup>+</sup> (Ref. [22], Figure S5). [c] 1.0 M **1**, 500 mM **2**, 25–50 mM catalyst, 20 °C, 12 h, > 90% yield. [d] Catalysts. [e] Circular dichroism at the first Cotton effect below 300 nm in toluene (CHCl<sub>3</sub>) (Figure 2). [f] Rate enhancement,  $\Delta E_a = -RT \ln(\nu_{\text{ini}}/\nu_{\text{ini}}^0)$ ;  $\nu_{\text{ini}}^0$  = initial velocity with **4**(S) in C<sub>6</sub>D<sub>6</sub> (25 mM cat.) [CDCl<sub>3</sub>/CD<sub>3</sub>OD (1:1) (50 mM cat.)]; negative: acceleration, positive: deceleration. [g] Enantiomeric excess in C<sub>6</sub>D<sub>6</sub> (25 mM cat.) [CDCl<sub>3</sub>/CD<sub>3</sub>OD (1:1) (50 mM cat.)]. [h] Diastereomeric ratio in C<sub>6</sub>D<sub>6</sub> (25 mM cat.) [CDCl<sub>3</sub>/CD<sub>3</sub>OD (1:1) (50 mM cat.)]. [i] Concentration for 50% inhibition by NBu<sub>4</sub>NO<sub>3</sub> in C<sub>6</sub>D<sub>6</sub> (50 mM cat., Figure 3). [j] 200 mM **8**, 2.0 M **2**, 40 mM (20 mol %) catalyst, [D<sub>8</sub>]THF, 20 °C, 10 h, > 90% total yield (A + D).<sup>[m]</sup> [k] Catalysts. [l] Rate enhancement for addition,  $\Delta E_a = -RT \ln(\nu_{\text{ini}}/\nu_{\text{ini}}^0)$ ,  $\nu_{\text{ini}}^0$  = initial velocity with **11** (Figure S4). [m] Yield of addition (A) product **9** / decarboxylation (D) product **10**. [n] With 2.0 M NBu<sub>4</sub>NO<sub>3</sub>. [o] With 2.0 M NBu<sub>4</sub>PF<sub>6</sub>. [p] In C<sub>6</sub>F<sub>6</sub>/C<sub>6</sub>D<sub>6</sub> (2:1).

anion- $\pi$  interactions has been demonstrated experimentally.<sup>[9]</sup>

Preliminary results with M062X/6-311G\*\*-optimized structures confirmed that the expanded PDI surface would be just perfect to comfortably accommodate **TS1** (Figure S6). To elaborate on these expectations experimentally, trifunctional catalysts **4**(S) with a remote proline on one side and a close glutamic acid on the other side of the  $\pi$  surface were synthesized (Figure 1, Schemes S1–S3, see SI for details). As with NDI homologs,<sup>[24]</sup> all NMR spectra of PDIs were complicated by the presence of rotamers (Figures S12–S20). This observation confirmed that *syn* and *anti* atropisomers do not have to be considered to interpret results on catalysis.

Catalytic activity was determined under routine conditions (Figures S1–S3).<sup>[9]</sup> From initial velocities of product formation, changes in activation energy  $\Delta E_a$ , i.e., relative transition-state stabilization were determined. Systematic solvent screening<sup>[24]</sup> revealed best results for [D<sub>6</sub>]benzene (Table 1, entry 1). Activities in the less interactive [D<sub>8</sub>]toluene were slightly weaker (Table S1). Slowest and fastest transformations obtained with the  $\pi$ -basic DMB and the  $\pi$ -acidic C<sub>6</sub>F<sub>6</sub>/C<sub>6</sub>D<sub>6</sub> (2:1; Tables S1; 1, entry 4) supported synergistic contributions from  $\pi$  stacking to weaken and strengthen anion- $\pi$  interactions, respectively.<sup>[25]</sup> In agreement with operational anion- $\pi$  interactions, increasing solvent polarity gave weaker results. For the continuation, the best and the worst solvent were maintained, i.e., C<sub>6</sub>D<sub>6</sub> and CDCl<sub>3</sub>/CD<sub>3</sub>OD (1:1; Table 1). In C<sub>6</sub>D<sub>6</sub>, the enantioselectivity obtained on PDI surfaces of **4**(S) was with 96% *ee* the best ever observed in molecular asymmetric anion- $\pi$  catalysis (Table 1, entry 1), the closest comparable value with NDIs is at 64% *ee*, the absolute record in the literature is at 91% *ee*.<sup>[24]</sup>

The diastereomeric catalyst **4**(R) was much slower and less stereoselective (Table 1, entry 5, Scheme S4). This significant response to inversion of the absolute configuration on the glutamate side provided experimental support that 1) the catalyst is indeed trifunctional,<sup>[9]</sup> 2) the reaction occurs on the  $\pi$ -acidic surface, and 3) the transition state on the expanded PDI surface in **4**(S) is favorable and thus sensitive to structural changes (Figure S6). Consistent with these important interpretations, elongation of the acid part with a glycine in **7**(R) (Figure 1, Scheme S4) increased activity with regard to the mismatched homolog **4**(R) without, however, reaching activity and selectivity of the matched **4**(S) by far (Table 1, entry 6).

In all tested solvents, rates and selectivities decreased with increasing reducibility from the matched **4**(S) with sulfides to **6**(S) with sulfones in the core (Tables S1; 1, entry 11). Decreasing activity with increasing reducibility from sulfide to sulfone suggested that, contrary to the planar NDIs, anion- $\pi$  catalysis with PDIs is determined by their twist rather than their reduction potentials. To assess PDI twisting, circular dichroism (CD) spectra of protected catalyst precursors of **4**(S) and **6**(S) were measured in apolar solvents (Figures 2, S7–S9). CD spectra of PDIs with sulfides in the core were almost silent (Figure 2c,d), whereas sulfones were CD active (Figure 2a,b), particularly in toluene (Figure 2a; Table 1, entries 1 and 11). This clear difference could support that the PDI twist indeed increases from sulfide **4**(S) to sulfone **6**(S). A negative exciton-coupled bisignate CD Cotton effect below 300 nm implied<sup>[26]</sup> an *M*-helical twist of the PDI plane of both **6**(S) and **6**(R), i.e., the absolute sense of twist is controlled by the chirality on the proline side (Figure 2a,b; Table 1, entries 11, 12). This deplanarization conceivably disturbed

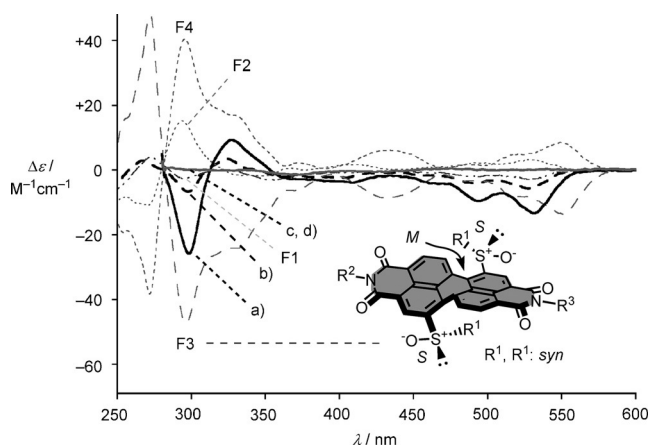


**Figure 2.** CD spectra of protected precursors of catalysts **6(S)** (a, b), **4(S)** (c, d) and **5(S, F1–F4)** in  $\text{CHCl}_3$  (b, d, F1–F4) and toluene (a, c), with the absolute configuration tentatively assigned to **5(S, F3)**.

the large quadrupole moment  $Q_{zz}$  of planar PDIs and thus weakened their catalytic activity. Theory predicts that, for example, twisting of the  $\pi$ -basic biphenyl from  $0^\circ$  to  $45^\circ$  reduces the negative  $Q_{zz}$  by quite remarkable 23%.<sup>[21]</sup>

For the intermediate **5(S)**, all four sulfoxide diastereomers<sup>[9]</sup> were separated by column chromatography and chiral-phase HPLC. Fractions 1 (F1) and F2 showed clearly different properties compared to F3 and F4, including absorption maxima and redox potentials (Table 1, entries 7–10). Their intense CD spectra suggested that F3 and F4 are the “matched” *syn* isomers with the alkyl substituents pointing to the same side of the aromatic surface (Figures 2, S7–S9). The *M* helicity in the CD spectrum below 300 nm implied that the absolute configuration of the sulfoxides in F3 is *S,S*. F4 thus should correspond to the *P,R,R* diastereomer, the less CD active F1 and F2 to the *anti* isomers with *S,R* and *R,S* sulfoxides. All four diastereomers of **5(S)** were different in catalysis but overall less active than sulfides **4(S)** and sulfones **6(S)** (Table 1, entries 7–10). This reduced activity of **5(S)** was understandable considering that the stereogenic centers at the edge of the PDI surfaces enhance and rigidify their twist.

The presence of 2.0 M tetrabutylammonium nitrate, the transition-state stabilization by **4(S)** decreased by  $\Delta E_a = +3.13 \text{ kJ mol}^{-1}$ , enantioselectivity dropped from 96% to 31% *ee*, and diastereoselectivity from 25:1 to 10:1 d.r. (Table 1, entry 2). The absence of similar inhibition with tetrabutylammonium hexafluorophosphate (except for presumably ion-pairing dominated<sup>[10]</sup> losses in diastereoselectivity; Table 1, entry 3), supported that nitrate inhibition originates from competitive nitrate– $\pi$  interactions.<sup>[10,11]</sup> Nitrate inhibition of sulfide **4(S)** with an  $\text{IC}_{50} = 125 \text{ mM}$  in  $[\text{D}_8]\text{toluene}$  exceeded the  $\text{IC}_{50} = 265 \text{ mM}$  obtained for sulfone **6(S)** significantly (Figure 3, Tables 1, entries 1, 11, S2). This difference supported that anion– $\pi$  interactions might indeed decrease with increasing twist of the  $\pi$  surface, despite a coinciding increase in reducibility.

The addition of malonic acid half thioesters (MAHTs) **8** to nitroolefin acceptor **2** is of interest because the addition product **9** is intrinsically disfavored compared to the less important decarboxylation product **10** (Figure 4). Anion– $\pi$

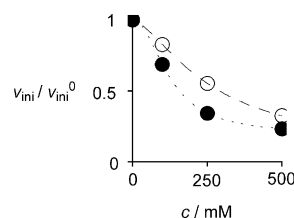


**Figure 3.** Initial velocity of formation of product **3** in the presence of substrates **1** and **2**, 10 mol% catalysts **4(S)** (●) or **6(S)** (○), and increasing concentrations of  $\text{TBANO}_3$ , with fit to Hill equation (Compare Table 1, entries 1, 11).

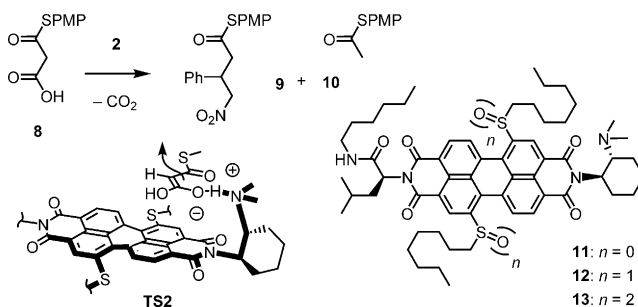


**Figure 4.** Anion– $\pi$  PDI catalysts **11–13** for enolate addition, with schematic representation of transition state **TS2** containing a stabilized planar tautomer that has to add before decarboxylation. PMP = *p*-methoxyphenyl.

catalysis on NDIs has been introduced to invert this selectivity, presumably by discriminating different tautomers of the conjugate bases of substrate **8** on the  $\pi$ -acidic surfaces (compare **TS2**).<sup>[8]</sup> To probe this enolate addition on PDIs, catalyst **11** was synthesized (Scheme S5, see the Supporting Information for details). Sulfide oxidation produced sulfoxide PDI **12** as an inseparable mixture of diastereomers, and sulfone PDI **13**. Evaluation under routine conditions<sup>[27]</sup> revealed that sulfide PDI **11** selectively catalyzes the unfavored enolate addition with an addition (**9**)/ decarboxylation (**10**) product ratio  $A/D = 1.8$  (Table 1, entry 1). With increasing reducibility of the  $\pi$  surface, selectivities decreased to  $A/D = 1.0$  for sulfoxide **12** and inverted back to  $A/D = 0.6$  for sulfone **13**, i.e., failed in “tortoise-and-hare” catalysis, that is to selectively catalyze that intrinsically disfavored enolate addition reaction (Table 1, entries 7, 11).<sup>[27]</sup> Rate enhancements for addition decreased correspondingly for sulfoxide **12** with  $\Delta E_a = +1.68 \text{ kJ mol}^{-1}$  and sulfone **13** with  $\Delta E_a = +2.22 \text{ kJ mol}^{-1}$  (Table 1, entries 1, 11). Results for sulfoxides **12** with intermediate reducibility should not be overestimated because of the presence of an inseparable diastereomeric mixture (Table 1, entry 7). More important was the most pronounced increase in activity ( $\Delta E_a = +2.22 \text{ kJ mol}^{-1}$ ) and inversion of selectivity (from  $A/D = 0.6$  to 1.8) with decreasing reducibility and twist from sulfone **13** to sulfide **11**. This finding was contrary to results with NDIs<sup>[27]</sup> and in agreement with the conclusions reached for enamine addition. These consistent trends were important because different to the trifunctional enamine catalysts **4–7**, anion– $\pi$  catalysts **11–13** for enolate addition are formally bifunctional and do not require communication between the PDI termini. Consistent



also with nitrate inhibition experiments for enamine addition, the results from bifunctional enolate addition catalysts thus provided additional experimental support that decreasing activities from sulfides to sulfones in the PDI core originate indeed from weakened  $Q_{zz}$ , i.e., anion- $\pi$  interactions, with increasing surface twisting, and not from topological mismatch or other sterical complications.

In summary, highlights from the explicit introduction of PDIs to anion- $\pi$  catalysis are sufficient space to comfortably accommodate transition states of appreciable size on the expanded  $\pi$ -acidic surface, giant quadrupole moments, and the highest enantioselectivity reported so far in anion- $\pi$  catalysis. Consistent trends from enamine and enolate addition, nitrate inhibition and CD spectroscopy indicate that deplanarization of the  $\pi$  surface inactivates anion- $\pi$  catalysts, and inactivation by deplanarization overcompensates activation by withdrawing substituents, i.e., electron deficiency. These results provide experimental support that for anion- $\pi$  interactions, quadrupole moments  $Q_{zz}$ , i.e., electrostatic interactions,<sup>[25]</sup> are more important than redox potentials, i.e., charge transfer. This conclusion is of general interest because anion- $\pi$  interactions on twisted aromatic surfaces are essentially unexplored.<sup>[28]</sup> With PDIs, deviations from planarity should thus be avoided, whereas, given their great  $Q_{zz}$ , the introduction of  $\pi$  acceptors *ortho* to the imides<sup>[20,29]</sup> appears most promising for the integration of unorthodox yet powerful anion- $\pi$  interactions into functional systems in the broadest sense.<sup>[5,11,30]</sup>

## Acknowledgments

We thank the NMR and the Sciences Mass Spectrometry (SMS) platforms for services, and the University of Geneva, the Swiss National Centre of Competence in Research (NCCR) Molecular Systems Engineering, the Swiss NCCR Chemical Biology, and the Swiss NSF for financial support.

**Keywords:** anion- $\pi$  interactions · homogeneous catalysis · perylenediimides · quadrupole moments · redox potentials

**How to cite:** *Angew. Chem. Int. Ed.* **2016**, 55, 14422–14426  
*Angew. Chem.* **2016**, 128, 14634–14638

- [1] a) A. Bauzá, T. J. Mooibroek, A. Frontera, *ChemPhysChem* **2015**, 16, 2496–2517; b) H. T. Chifotides, K. R. Dunbar, *Acc. Chem. Res.* **2013**, 46, 894–906; c) D.-X. Wang, M.-X. Wang, *Chimia* **2011**, 65, 939–943; d) P. Ballester, *Acc. Chem. Res.* **2013**, 46, 874–884.
- [2] C. R. Kennedy, S. Lin, E. N. Jacobsen, *Angew. Chem. Int. Ed.* **2016**, 55, 12596–12624; *Angew. Chem.* **2016**, 128, 12784–12814.
- [3] a) D. Quiñonero, C. Garau, C. Rotger, A. Frontera, P. Ballester, A. Costa, P. M. Deyà, *Angew. Chem. Int. Ed.* **2002**, 41, 3389–3392; *Angew. Chem.* **2002**, 114, 3539–3542; b) M. Mascal, A. Armstrong, M. D. Bartberger, *J. Am. Chem. Soc.* **2002**, 124, 6274–6276; c) I. Alkorta, I. Rozas, J. Elguero, *J. Am. Chem. Soc.* **2002**, 124, 8593–8598; d) H.-J. Schneider, F. Werner, T. Blatter, *J. Phys. Org. Chem.* **1993**, 6, 590–594.
- [4] V. Gorteau, G. Bollot, J. Mareda, A. Perez-Velasco, S. Matile, *J. Am. Chem. Soc.* **2006**, 128, 14788–14789.
- [5] Y. Zhao, Y. Cotellet, N. Sakai, S. Matile, *J. Am. Chem. Soc.* **2016**, 138, 4270–4277.
- [6] a) M. Giese, M. Albrecht, K. Rissanen, *Chem. Commun.* **2016**, 52, 1778–1795; b) Q. He, Y.-F. Ao, Z.-T. Huang, D.-X. Wang, *Angew. Chem. Int. Ed.* **2015**, 54, 11785–11790; *Angew. Chem.* **2015**, 127, 11951–11956; c) S. T. Schneebeli, M. Frascioni, Z. Liu, Y. Wu, D. M. Gardner, N. L. Strutt, C. Cheng, R. Carmieli, M. R. Wasielewski, J. F. Stoddart, *Angew. Chem. Int. Ed.* **2013**, 52, 13100–13104; *Angew. Chem.* **2013**, 125, 13338–13342.
- [7] Y. Zhao, Y. Domoto, E. Orentas, C. Beuchat, D. Emery, J. Mareda, N. Sakai, S. Matile, *Angew. Chem. Int. Ed.* **2013**, 52, 9940–9943; *Angew. Chem.* **2013**, 125, 10124–10127.
- [8] a) Y. Zhao, S. Benz, N. Sakai, S. Matile, *Chem. Sci.* **2015**, 6, 6219–6223; b) F. N. Miros, Y. Zhao, G. Sargsyan, M. Pupier, C. Besnard, C. Beuchat, J. Mareda, N. Sakai, S. Matile, *Chem. Eur. J.* **2016**, 22, 2648–2657.
- [9] Y. Zhao, Y. Cotellet, A.-J. Avestro, N. Sakai, S. Matile, *J. Am. Chem. Soc.* **2015**, 137, 11582–11585.
- [10] L. Liu, Y. Cotellet, A.-J. Avestro, N. Sakai, S. Matile, *J. Am. Chem. Soc.* **2016**, 138, 7876–7879.
- [11] Y. Cotellet, V. Lebrun, N. Sakai, T. R. Ward, S. Matile, *ACS Cent. Sci.* **2016**, 2, 388–393.
- [12] a) A. Berkessel, S. Das, D. Pekel, J.-M. Neudörfl, *Angew. Chem. Int. Ed.* **2014**, 53, 11660–11664; *Angew. Chem.* **2014**, 126, 11846–11850; b) K. S. Lee, J. R. Parquette, *Chem. Commun.* **2015**, 51, 15653–15656; c) J. V. Alegre-Requena, E. Marqués-López, R. P. Herrera, *Adv. Synth. Catal.* **2016**, 358, 1801–1809; d) A. Lattanzi, C. De Fusco, A. Russo, A. Poater, L. Cavallo, *Chem. Commun.* **2012**, 48, 1650–1652; e) P. Phuengphai, S. Youngme, I. Mutikainen, J. Reedijk, *Inorg. Chem. Commun.* **2012**, 24, 129–133; f) C. Estarellas, A. Frontera, D. Quiñonero, P. M. Deyà, *Angew. Chem. Int. Ed.* **2011**, 50, 415–418; *Angew. Chem.* **2011**, 123, 435–438.
- [13] M. Al Kobaisi, S. V. Bhosale, K. Latham, A. M. Raynor, S. V. Bhosale, *Chem. Rev.* **2016**, DOI: 10.1021/acs.chemrev.6b00160.
- [14] a) F. Würthner, C. R. Saha-Möller, B. Fimmel, S. Ogi, P. Leowanawat, D. Schmidt, *Chem. Rev.* **2016**, 116, 962–1052; b) V. M. Blas-Ferrando, J. Ortiz, K. Ohkubo, S. Fukuzumi, F. Fernandez-Lazaro, A. Sastre-Santos, *Chem. Sci.* **2014**, 5, 4785–4793.
- [15] C. M. Rojas, J. Rebek, Jr., *J. Am. Chem. Soc.* **1998**, 120, 5120–5121.
- [16] Y. Zhao, C. Beuchat, Y. Domoto, J. Gajewy, A. Wilson, J. Mareda, N. Sakai, S. Matile, *J. Am. Chem. Soc.* **2014**, 136, 2101–2111.
- [17] A. Perez-Velasco, V. Gorteau, S. Matile, *Angew. Chem. Int. Ed.* **2008**, 47, 921–923; *Angew. Chem.* **2008**, 120, 935–937.
- [18] R. E. Dawson, A. Hennig, D. P. Weimann, D. Emery, V. Ravikumar, J. Montenegro, T. Takeuchi, S. Gabutti, M. Mayor, J. Mareda, C. A. Schalley, S. Matile, *Nat. Chem.* **2010**, 2, 533–538.
- [19] See TOC graphic for an EPS image (MP2/6-311+ + G\*\*//M062X/6-311G\*\*), projected on the 0.008 au electron density isosurface and color-coded between –0.02 au (red, electron rich) and 0.077 au (blue, electron poor).
- [20] G. Battagliarin, Y. Zhao, C. Li, K. Müllen, *Org. Lett.* **2011**, 13, 3399–3401.
- [21] A. Chablo, D. W. J. Cruckshank, A. Hinchliffe, R. W. Munn, *Chem. Phys. Lett.* **1981**, 78, 424–428.
- [22] F. N. Miros, S. Matile, *ChemistryOpen* **2016**, 5, 219–226.
- [23] J. Lubkoll, H. Wennemers, *Angew. Chem. Int. Ed.* **2007**, 46, 6841–6844; *Angew. Chem.* **2007**, 119, 6965–6968.
- [24] M. Akamatsu, S. Matile, *Synlett* **2016**, 1041–2046.
- [25] A. Frontera, D. Quiñonero, P. M. Deyà, *Wiley Interdiscip. Rev.: Comput. Mol. Sci.* **2011**, 1, 440–459.
- [26] a) M. M. Safont-Sempere, P. Osswald, M. Stolte, M. Grüne, M. Renz, M. Kaupp, K. Radacki, H. Braunschweig, F. Würthner, J.

- Am. Chem. Soc.* **2011**, *133*, 9580–9591; b) N. Berova, K. Nakanishi, *Circular Dichroism: Principles and Applications*, Wiley-VCH, New York, **2000**.
- [27] Y. Cotellet, S. Benz, A.-J. Avestro, T. R. Ward, N. Sakai, S. Matile, *Angew. Chem. Int. Ed.* **2016**, *55*, 4275–4279; *Angew. Chem.* **2016**, *128*, 4347–4351.
- [28] A. Campo-Cacharron, E. M. Cabaleiro-Lago, I. Gonzalez-Veloso, J. Rodríguez-Otero, *J. Phys. Chem. A* **2014**, *118*, 6112–6124.
- [29] a) S. Nakazono, Y. Imazaki, H. Yoo, J. Yang, T. Sasamori, N. Tokitoh, T. Cedric, H. Kageyama, D. Kim, H. Shinokubo, A. Osuka, *Chem. Eur. J.* **2009**, *15*, 7530–7533; b) S. W. Eaton, L. E. Shoer, S. D. Karlen, S. M. Dyar, E. A. Margulies, B. S. Veldkamp, C. Ramanan, D. A. Hartzler, S. Savikhin, T. J. Marks, M. R. Wasielewski, *J. Am. Chem. Soc.* **2013**, *135*, 14701–14712.
- [30] a) B. Baumeister, N. Sakai, S. Matile, *Org. Lett.* **2001**, *3*, 4229–4232; b) N. Sakai, S. Matile, *J. Am. Chem. Soc.* **2011**, *133*, 18542–18545.

Received: September 9, 2016

Published online: October 14, 2016